ELSEVIER

Fusion Engineering and Design 65 (2003) 285–301

Fusion Engineering and Design

www.elsevier.com/locate/fusengdes

ARIES-ST safety design and analysis

H.Y. Khater [a,*], E.A. Mogahed [a], D.K. Sze [b], M.S. Tillack [c], X.R. Wang [c], The ARIES Team

[a] *Fusion Technology Institute, University of Wisconsin-Madison, Madison, WI, USA*
[b] *Argonne National Laboratory, Argonne, IL, USA*
[c] *Fusion Energy Research Program, University of California, San Diego, CA, USA*

Abstract

Activation and safety analyses were performed for the ARIES-ST design. The ARIES-ST power plant includes a water-cooled copper centerpost. The first wall and shield are made of low activation ferritic steel and cooled with helium. The blanket is also made of ferritic steel with SiC inserts and $Li_{17}Pb_{83}$ breeder. The divertor plate is made of low activation ferritic steel and uses a tungsten brush as plasma facing component. The power plant has a lifetime of 40 full power years (FPY). However, the centerpost, first wall, inboard shield and blanket were assumed to be replaced every 2.86 FPY. Neutron transmutation of copper resulted in the production of several nickel, cobalt and zinc isotopes. The production of these isotopes resulted in an increase of the time-space average electrical resistivity of the centerpost by about 6% after 2.86 FPY. All of the plant components met the limits for disposal as Class C low-level waste. The off-site doses produced at the onset of an accident are caused by the mobilization of the radioactive inventory present in the plant. Analysis of a loss of coolant accident (LOCA) indicated that the centerpost would reach a maximum temperature of about 1000 °C during the accident. In the meantime, the first wall and shield would reach a maximum temperature of about 800 °C. A similar divertor LOCA analysis indicated that the front tungsten layer would also reach a maximum temperature of about 800 °C. The calculated temperature profiles and available oxidation-driven volatility experimental data were used to calculate the dose at the site boundary under conservative release conditions. The current design produces an effective whole body early dose of 1.88 mSv at the site boundary. In addition, a divertor disruption would only produce an effective whole body early dose of 7.68 μSv at the site boundary.

1. Introduction

ARIES-ST is a low-aspect-ratio spherical torus power plant, which is one of several fusion power plant designs being assessed within the ARIES project. The ARIES-ST power plant [1] produces a 1000 MW of net electric power and is assumed to operate for 40 full power years (FPY). The plant includes a water-cooled, DS GlidCop Al-15 copper centerpost. The first wall and shield are made of low activation ferritic steel (9Cr-2WVTa) and cooled with helium [2]. The blanket is also made

* Corresponding author. Tel.: +1-650-926-2048; fax: +1-650-926-3569.
E-mail address: khater@slac.stanford.edu (H.Y. Khater).

0920-3796/03/$ - see front matter © 2002 Elsevier Science B.V. All rights reserved.
PII: S0920-3796(02)00307-1

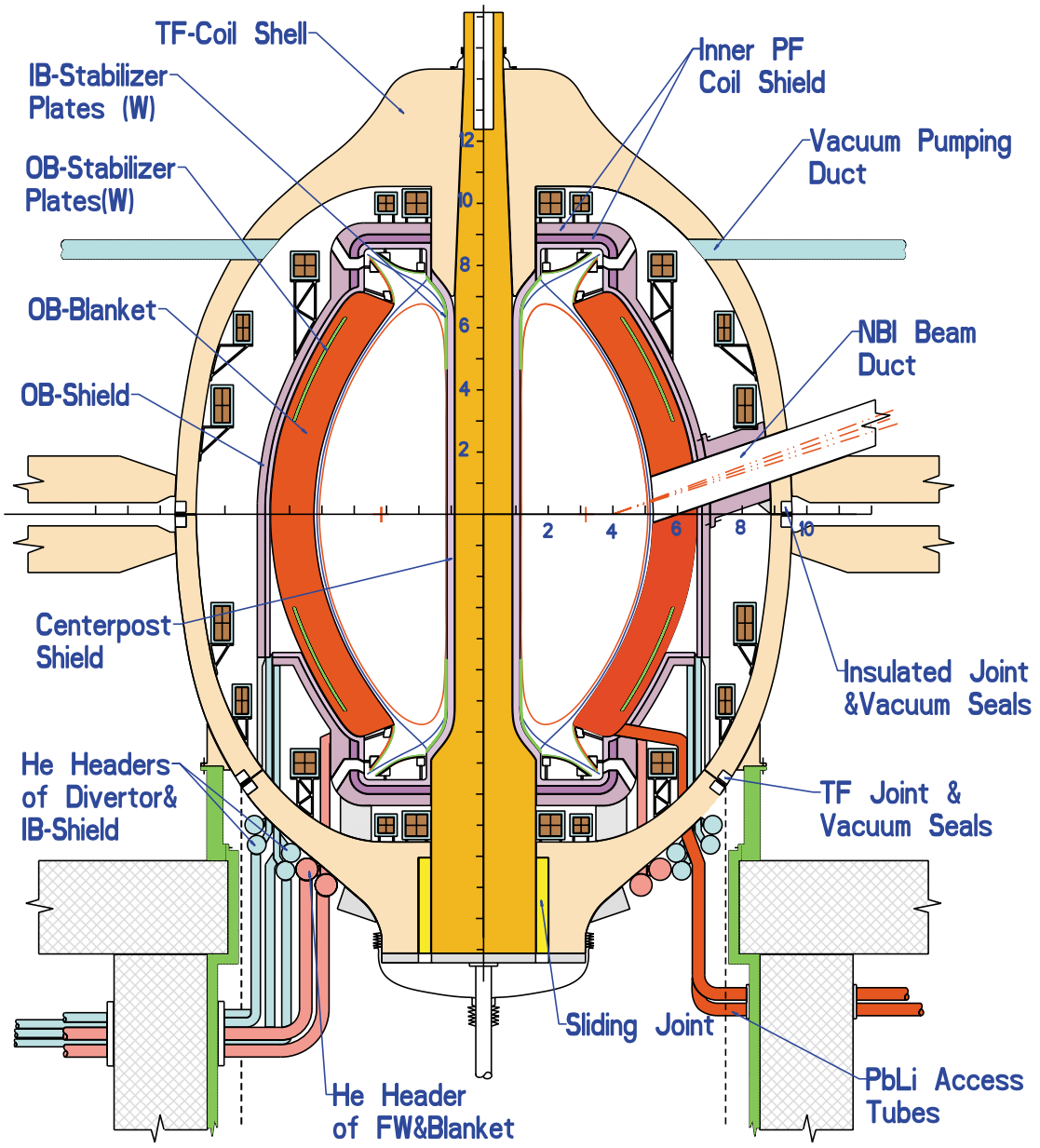

Fig. 1. Elevation view of the ARIES-ST power core.

of ferritic steel with SiC inserts and $Li_{17}Pb_{83}$ breeder. Fig. 1 shows an elevation view of the ARIES-ST power core. As shown in Fig. 2, the design utilizes a divertor with a steel back plate and uses a tungsten brush as plasma facing component (PFC). Activation analysis was performed assuming average neutron wall loadings of 2.1 and 4.6 MW/m^2 at the inboard and outboard first wall, respectively. In addition, the average neutron wall loading at the inner divertor plate is 0.9 MW/m^2. The neutron wall loadings are the limiting factors for the lifetime of the different

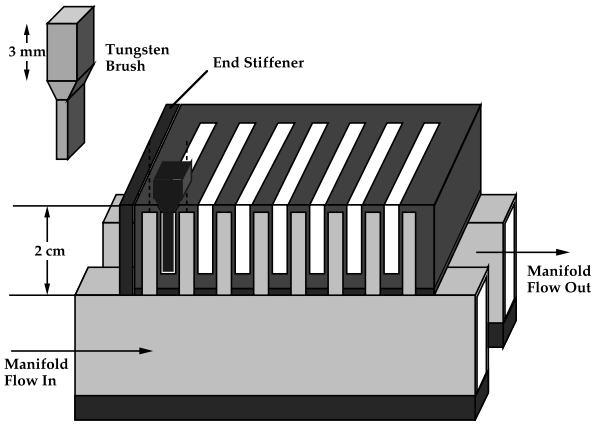

Fig. 2. Configuration of the slotted duct divertor plate.

components of the power plant. The centerpost, first wall, inboard shield and blanket were assumed to survive for 2.86 FPY [3]. The divertor plate and manifold were assumed to have a lifetime of 2.86 FPY. The divertor shield was assumed to stay in place for 40 FPY due to the fact that it is exposed to a lower neutron environment. The activity and decay heat were calculated as a function of time following shutdown. Calculation of the structure activity is needed to evaluate the potential impact of a radioactive inventory release at the onset of an accident. Results of the decay heat calculation are used to examine the thermal response of the plant structure following a loss of coolant accident (LOCA). The waste disposal ratings (WDR) of the different plant components at the end of their lifetimes were also evaluated. The WDR is needed to determine if a given structure component would satisfy the regulatory criteria for shallow land burial as low-level waste (LLW).

A strong emphasis has been given to the environment and safety issues in the ARIES-ST power plant design. Low activation ferritic steel (9Cr-2WVTa) has been used in the blanket and shield to avoid a high level of induced radioactivity. Similarly, the use of $Li_{17}Pb_{83}$ as a breeder eliminates the hazard posed by the energy producing chemical reactions usually associated with the use of lithium and hence reduces the risk of mobilizing the radioactive inventory present in the plant. The methodology used in this analysis dose not depend on the probability of accident initiating scenarios. In accordance with previous ARIES safety analyses, we have rather adopted the principle of considering a severe accident scenario, while maintaining integrity of all containment barriers during such an accident. To evaluate the possible radiological hazard to the public, we used a two step approach in calculating the possible off-site dose. The first step in our approach is the identification of the sources and locations of the radioactive inventories inside the plant building. However, since the existence of radioactivity does not in itself represent a safety hazard, the second step in our approach was to consider a set of pessimistic accident scenarios for mobilizing and releasing the radioactive inventory. A major goal of the ARIES-ST design has been achieving the highest level of safety while maintaining its economic attractiveness. Taking this into account, the design aimed at achieving the following goals:

1) Minimizing the increase in the centerpost resistivity.
2) Disposal of the plant structure as LLW.
3) Significantly reducing the off-site doses from routine release of tritium during operation.
4) Minimizing the level of off-site doses at the site boundary following an accident.

In this paper, it is shown that the first goal could be achieved by adequate shielding of the centerpost. The other goals could be achieved by using low activation materials in the first wall and shield of the plant and proper design of the heat exchanger to minimize the amount of routine tritium release. The 9Cr-2WVTa ferritic steel was selected because it produces a low level of long-term radioactivity and acceptable levels of short and intermediate-term radioactivity. The disposal of the structure as LLW is dependent on producing low levels of long-term radioactivity. On the other hand, off-site doses during an accident are dominated by nuclides with short and intermediate lifetimes. In addition, nuclides with intermediate lifetimes are the major contributors to the decay heat and hence, the temporal variation of the structure temperature during an accident.

2. Calculational procedure

The neutron flux used for the activation calculations was generated by the one-dimensional discrete ordinates neutron transport code ONEDANT [4]. A 46-group neutron and 21-group gamma coupled cross section library, based on FENDL1.0 [5]. The analysis uses a P_3 approximation for the scattering cross sections and S_8 angular quadrature set. The plant structure calculations used toroidal cylindrical geometry models with the inboard and outboard sides modeled simultaneously. The average neutron wall loading on the inboard and outboard sides are 2.1 and 4.6 MW/m^2 [3], respectively. The average neutron wall loading at the inner divertor plate is 0.9 MW/m^2. The activation analysis was performed using the latest version of the activation code DKR-PULSAR2.0 [6]. The code combined the neutron flux with the FENDL/A-2.0 data library [7] to calculate the activity and decay heat generated in the different regions of the plant. The plant was assumed to operate continuously for 40 FPY. The centerpost, first wall, inboard shield and blanket were assumed to be replaced every 2.86 FPY. The divertor plate and manifold were assumed to have a lifetime of 2.86 FPY. The divertor shield was assumed to stay in place for 40 FPY. The decay gamma source produced by the DKR-PULSAR2.0 code was used with the adjoint neutron flux to calculate the biological dose rates after shutdown using the DOSE code [6]. The dose rate calculations were performed at different locations inside the containment. The structure activation results were utilized in a radwaste classification. The decay heat results were used in a LOCA analysis. The structure and the $Li_{17}Pb_{83}$ breeder activation results were used in the off-site dose calculations following the LOCA. The activation results have also been utilized in the off-site dose calculation. The off-site doses are produced by the accidental release of the radioactive inventory from the containment building assuming the worst case weather conditions. Finally, the EPA code AIRDOS-PC [8] has been used to estimate the off-site dose due to the routine release of tritium. The materials used in the different regions of the plant are presented in Table 1.

Table 1
Materials used in the activation analysis of ARIES-ST

Component	Composition
Centerpost	85% GlidCop Cu and 15% water
Inboard shield	80% Ferritic steel and 20% He
Inboard first wall	26% Ferritic steel and 74% He
Outboard first wall	40% Ferritic steel and 60% He
Outboard blanket	6% Ferritic steel, 6% He, 12% SiC, and 76% $Li_{17}Pb_{83}$
Outboard shield	30% Ferritic steel and 70% He
Divertor tungsten brush	100% W
Divertor coolant channel	50% W and 50% He
Divertor back plate	100% Ferritic steel
Divertor manifold	67% Ferritic steel and 33% He
Divertor high temperature shield	15% Ferritic steel, 80% WC, and 5% water
Divertor low temperature shield	15% Ferritic steel, 70% WC, and 15% water

3. Activation analysis

3.1. Activity and decay heat

After 2.86 FPY, the total activity induced in the centerpost is 4430 MCi and drops to 994 MCi in 1 day and 2.7 MCi in 1 week. In the meantime, the total decay heat induced in the centerpost is 12.25 MW and drops to 1.87 MW within a day. The decay heat induced in the centerpost is dominated by the two copper isotopes ^{64}Cu ($T_{1/2} = 12.7$ h) and ^{66}Cu ($T_{1/2} = 5.1$ m). The dominant nuclides at 1 week following shutdown are ^{60}Co ($T_{1/2} = 5.27$ yr) and ^{64}Cu. The total activity induced in the inboard shield and first wall at shutdown is 959 MCi and drops to 594 MCi in 1 day and 501 MCi after 1 week. At shutdown, the decay heat amounts to 5.14 MW and drops to 0.56 MW within a week. The decay heat at shutdown is dominated by ^{56}Mn ($T_{1/2} = 2.578$ h) and ^{187}W ($T_{1/2} = 23.9$ h). At 1 day following shutdown, the decay heat induced in the inboard shield and first wall is dominated by ^{54}Mn ($T_{1/2} = 312.2$ d) and ^{56}Mn.

The amounts of activity and decay heat induced in the outboard first wall/blanket structure and shield after 2.86 FPY are 2800 MCi and 19.2 MW, respectively. The activity and decay heat drop to

1552 MCi and 1.25 MW within a week from shutdown. Most of the activity and decay heat are induced in the ferritic steel part of the structure and dominated by the same nuclides as in the inboard first wall and shield. The amount of activity induced in the $Li_{17}Pb_{83}$ blanket at shutdown is 5252 MCi. Due to the rapid decay of ^{207m}Pb ($T_{1/2} = 0.8$ s), the activity of $Li_{17}Pb_{83}$ drops to only 140 MCi within a day from shutdown.

The tungsten plasma facing part of the divertor has a total induced activity and decay heat after 2.86 FPY of 546 MCi and 0.8 MW, respectively. The dominant nuclides at shutdown are ^{187}W ($T_{1/2} = 23.9$ h), ^{185}W ($T_{1/2} = 74.8$ d), and ^{183m}W($T_{1/2} = 5.15$ s). After 1 day following shutdown ^{187}W, ^{185}W, and ^{181}W ($T_{1/2} = 121.2$ d) dominate the activity and decay heat induced in the tungsten layer. The amount of activity generated in the divertor back plate at shutdown is 129 MCi and decays to 79 MCi within a week. The decay heat generated in the back plate drops from 0.69 to 0.082 MW during the first day following shutdown.

3.2. Change in centerpost electrical resistivity

Interactions between high-energy neutrons and the copper centerpost lead to the production of several nickel, cobalt, and zinc isotopes as transmutation products. Production of these isotopes leads to an increase in the centerpost electrical resistivity. The centerpost resistivity increases linearly with the increase in time of operation. Increase in the centerpost resistivity would lead to an increase in the recirculating power and lower net efficiency. The following are the most important reactions:

- $^{63}Cu(n,2n)^{62}Cu(\beta^+)^{62}Ni$, $^{65}Cu(n,2n)^{64}Cu(\beta^+)^{64}Ni$, and $^{63}Cu(n,\gamma)^{64}Cu(\beta^+)^{64}Ni$
- $^{63}Cu(n,\gamma)^{64}Cu(\beta^-)^{64}Zn$, $^{65}Cu(n,2n)^{64}Cu(\beta^-)^{64}Zn$, and $^{65}Cu(n,\gamma)^{66}Cu(\beta^-)^{66}Zn$
- $^{63}Cu(n,\gamma)^{64}Cu(n,n\alpha)^{60}Co$, and $^{65}Cu(n,2n)^{64}Cu(n,n\alpha)^{60}Co$

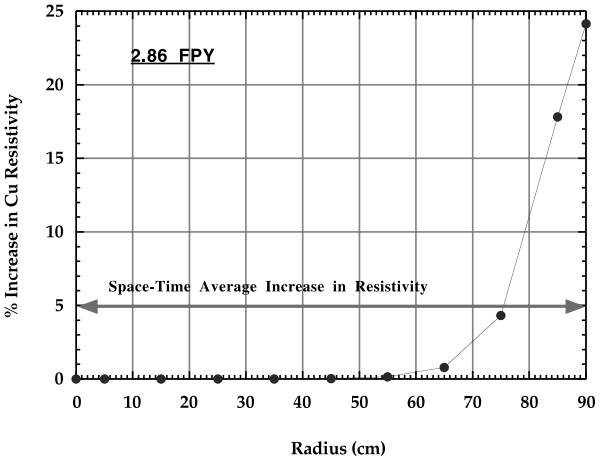

Fig. 3. Radial distribution of the percentage increase in the centerpost resistivity.

Fig. 3 shows the radial distribution of the percentage increase in the centerpost resistivity. As shown in the figure, the outermost 30 cm of the 80 cm-thick centerpost exhibits the bulk of transmutation. This is due to the fact that the change in the copper transmutation is mostly due to the production of the ^{64}Ni isotope. As already shown, ^{64}Ni is mostly produced via high-energy threshold reactions. The electric current will redistribute within the centerpost to avoid the region with high resistivity. The space-time average increase in resistivity over the entire centerpost is about 6%, which is considered a tolerable value.

3.3. Biological dose rates

Biological dose rate calculations were performed at selected locations in the space between the centerpost and the back of the inboard shield, and in the space between the outboard blanket and the magnet. Fig. 4 shows the calculated dose rates as a function of time following shutdown. At shutdown, the biological dose rate in the space between the centerpost and the back of the inboard shield is 4.57×10^7 mSv/h. The dose is dominated by the ^{56}Mn ($T_{1/2} = 2.578$ h) and ^{187}W ($T_{1/2} = 23.9$ h) isotopes produced from the ferritic steel component of the inboard shield, and ^{66}Cu ($T_{1/2} = 5.1$ m) produced from the copper centerpost. One day following shutdown the dose rate

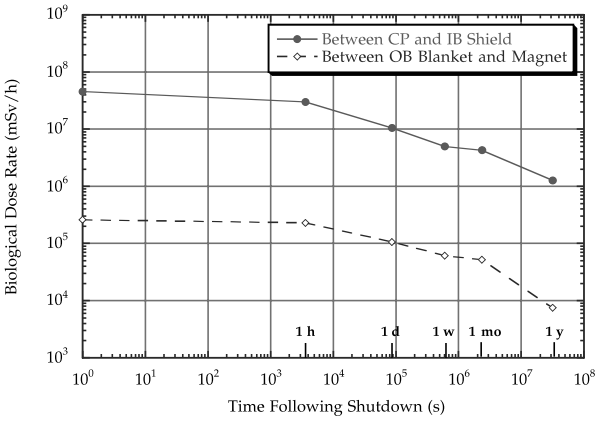

Fig. 4. Biological dose rates following shutdown.

drops to 1.05×10^7 mSv/h. The two isotopes, ^{187}W ($T_{1/2} = 23.9$ h) and ^{182}Ta ($T_{1/2} = 114.43$ d), dominate the dose rate at that time. ^{187}W and ^{182}Ta are produced in the inboard shield. The dose rate continues to be high for years following shutdown. After 1 year, the biological dose rate is 1.27×10^6 mSv/h and is dominated by ^{60}Co ($T_{1/2} = 5.27$ yr) produced from the centerpost, and ^{54}Mn ($T_{1/2} = 312.2$ d) and ^{182}Ta produced from the inboard shield.

As shown in the figure, the biological dose rates in the space between the outboard blanket and the magnet continues to be high. For the most part these dose rates are also dominated by the same nuclides mentioned before. However, all of these nuclides are generated in the ferritic steel component of the outboard blanket. Since the high biological dose rates continue for several years following shutdown, only remote maintenance is feasible anywhere inside the ARIES-ST building.

3.4. Radwaste classification

The radwaste of the different regions of the plant were evaluated according to both the NRC 10CFR61 [9] and Fetter [10] waste disposal concentration limits (WDL). The 10CFR61 regulations assume that the waste disposal site will be under administrative control for 100 years. The dose at the site to an inadvertent intruder after the 100 years is limited to less than 500 mrem/yr. The WDR is defined as the sum of the ratio of the concentration of a particular isotope to the maximum allowed concentration of that isotope taken over all isotopes and for a particular class. If the calculated WDR = 1 when Class A limits are used, the radwaste should qualify for Class A segregated waste. The major hazard of this class of waste is to individuals who are responsible for handling it. Such waste is not considered to be a hazard following the loss of institutional control of the disposal site. If the WDR > 1 when Class A WDL are used but WDR $\leqslant$ 1 when Class C limits are used, the waste is termed Class C intruder waste. It must be packaged and buried such that it will not pose a hazard to an inadvertent intruder after the 100 years institutional period is over. Class C waste is assumed to be stable for 500 years. Using Class C limits, a WDR > 1 implies that the radwaste does not qualify for shallow land burial. Fetter developed a modified version of the NRC's intruder model to calculate waste disposal limits for a wider range of long-lived radionuclides which are of interest for fusion researchers than the few that currently exist in the current 10CFR61 regulations. Fetter's model included more accurate transfer coefficients and dose conversion factors. However, while the NRC model limits the whole body dose to 500 mrem or the dose to any single organ (one of seven body organs) to 1.5 rem, Fetter limits are based on the maximum dose to the whole body only.

Specific activities calculated by the DKR-PULSAR2.0 code were used to calculate the WDR.

Table 2
Waste disposal ratings using 10CFR61 limits

Zone	Life (FPY)	WDR	Dominant nuclides
Centerpost	2.86	0.88	^{63}Ni
Inboard shield	2.86	0.17	^{94}Nb
Inboard first wall	2.86	0.2	^{94}Nb
Outboard first wall	2.86	0.26	^{94}Nb
Outboard blanket	2.86	0.021	^{94}Nb
Outboard shield	2.86	3.7×10^{-3}	^{94}Nb
Divertor plate	2.86	0.18	^{94}Nb
Divertor shield	40	0.012	^{94}Nb, ^{14}C

Table 3
Waste disposal ratings using fetter limits

Zone	Life (FPY)	WDR	Dominant nuclides
Centerpost	2.86	0.4	^{108m}Ag
Inboard shield	2.86	0.69	^{192m}Ir, ^{94}Nb
Inboard first wall	2.86	0.55	^{192m}Ir ^{94}Nb
Outboard first wall	2.86	0.65	^{192m}Ir, ^{94}Nb
Outboard blanket	2.86	0.049	^{192m}Ir, ^{94}Nb
Outboard shield	2.86	0.015	^{192m}Ir
Divertor plate	2.86	0.49	^{94}Nb, ^{108m}Ag
Divertor shield	40	0.017	^{94}Nb, ^{192m}Ir

The WDR for the 10CFR61 and Fetter limits are shown in Table 2 and Table 3. Results in the tables are given for compacted wastes. Compacted waste corresponds to crushing the solid waste before disposal and thus disallowing artificial dilution of activity. The Class C WDR values were calculated after a 1-year cooling period. As shown in Table 2, according to the 10CFR61 limits, the centerpost WDR is dominated by ^{63}Ni, which is produced via the ^{63}Cu(n, p) reaction. Since this reaction is a high-energy threshold reaction, providing extra shielding on the inboard side could reduce the amount of ^{63}Ni generated in the centerpost further. On the other hand, ^{94}Nb, produced from the 0.5 wppm niobium impurities in the 9Cr-2WVTa steel, is the dominant source of waste hazard in the first wall, blanket and shield. As shown in Table 3, ^{108m}Ag produced from the 20 wppm silver impurities contained in the GlidCop Al-15 copper alloy, is the major waste hazard in the centerpost according to Fetter limits. In addition to ^{94}Nb, ^{192m}Ir is the other waste hazard associated with ferritic steel. These results show that the waste classification of the centerpost is controlled by its 10CFR61 WDR as it is entirely due to direct transmutation of copper rather than impurities included in the Cu alloy. All other WDR could be limited by controlling the level of impurities in the copper and steel alloys regardless of the waste disposal limits used. Similarly, as shown in the tables, the niobium and silver impurities in the divertor tungsten PFC and ferritic steel back plate are entirely responsible for the waste hazard of the divertor plate.

4. Loss of coolant accident analysis

The goal of this analysis is to determine the temperature history of the different plant components as a function of time following a LOCA. LOCA occurs when one or more supply tubes outside the plant are damaged or ruptured, preventing the coolant from reaching the first wall or PFCs. Even though neutron heating is absent, the lack of coolant in the coolant channels causes the temperature to rise in various sections of the blanket and shield due to decay heat. For ARIES-ST, it is assumed that the plasma is immediately quenched and the chamber components begin to increase in temperature due to the decay heat generated. Due to the large difference between the time scale of plasma shutdown ≈ 1 ms and the loss of coolant or loss of flow (several minutes-hours), it is assumed that the plasma is immediately quenched at the onset of the LOCA/LOFA and the chamber components' temperature begins to increase due to the decay heat generated (worst case scenario). The thermal response of the blanket, shield, and divertor following a LOCA is determined by the analysis of an axi-symmetric (R, ϕ) finite element model for the entire power plant (Fig. 5). This analysis examines the thermal behavior of the in-vessel components to determine the temperature profiles as a function of time following LOCA.

In this LOCA analysis, the centerpost is made of copper with empty coolant channels. The cross-sectional area of the empty coolant channels represents 15% of the total centerpost cross-sectional area. The same conditions are applicable for the rest of the power plant. The outer shell of the toroidal field (TF) magnet is made of aluminum and is connected to the bus-bars at the midplane. This analysis allowed conduction up/down the centerpost, and in the TF coil outer leg winding pack (WP). The centerpost and the TF coil outer leg WP are assumed to be connected to an ultimate heat sink at a temperature of 35 °C. The present centerpost/WP design is intimately connected to very large bus-bars (an ultimate heat sink). The centerpost is connected to the TF coil outer legs at both ends of the centerpost.

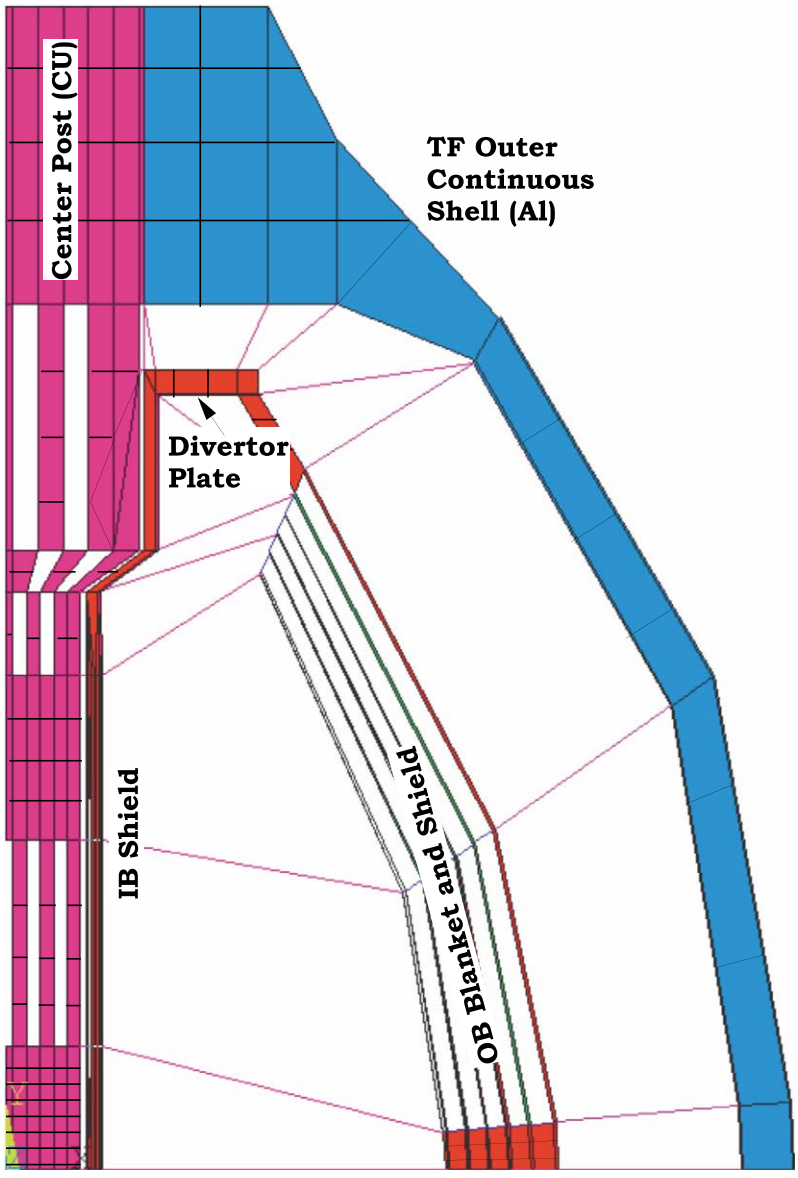

Fig. 5. Finite element model for the inboard and outboard of ARIES-ST.

4.1. Methodology

In order to perform the ARIES-ST LOCA analysis, several assumptions had to be made. The assumptions for the accident conditions were:

(1) Coolants are drained from all the blanket/shield sectors as well as the divertor plate leaving the coolant channels empty and making it possible for coolant channel surfaces to radiate to each other.

(2) The plasma is quenched instantaneously upon the onset of a LOCA. An appropriate shutdown mechanism must be in place for this to happen. If the coolant leaks into the chamber that would cause an immediate plasma shutdown while the coolant is still running. On the other hand, if it

takes 10 s for the plasma to be deliberately shut down after the complete coolant loss, the heat generated amounts to 1% of the integrated after-heat in the first week after LOCA. Although this does not appear to be very much, the immediate effect on the first wall during that 10 s could be significant.

(3) All facing surfaces radiate to each other.

(4) Both inboard and outboard blanket/shields are solved interactively and can therefore radiate to each other across the plasma space.

(5) Heat transfer across the gaps is by thermal radiation and partially by thermal conduction. In the gaps a certain percentage of the facing area is assumed to have connecting structure for internal support and can, therefore, also conduct heat.

(6) Thermal emissivity is taken as 0.5 for all surfaces.

(7) The massive copper bus-bars are considered as ultimate heat sinks at a constant temperature of 35 °C.

(8) Temperature dependent thermo-physical properties are used for all the materials.

(9) The material properties of the different zones in the radial build have been adjusted (linearly proportional to volumetric ratio) to preserve the density, heat capacitance and thermal conductivity of the actual composition.

4.2. Modeling and boundary conditions

An axi-symmetric model is employed for finite element analysis. The commercial finite element code ANSYS 5.4 is used in this analysis [11]. The finite element model used in the analysis is shown in Fig. 5. The only thermal loads considered in this analysis are those generated as decay heat at the onset of a LOCA. The external surface of the plant is considered as an adiabatic boundary. The copper in the centerpost is thermally conducting to the aluminum outer shell of the TF coils. The TF outer shell is connected to an ultimate heat sink through the massive conduction bars. The average decay heat variations in the outboard and inboard sides near the midplane are shown in Fig. 6 for the first week after shutdown. Fig. 7 shows the change in the average decay heat behind the inboard tungsten stabilizer plate at the inboard top

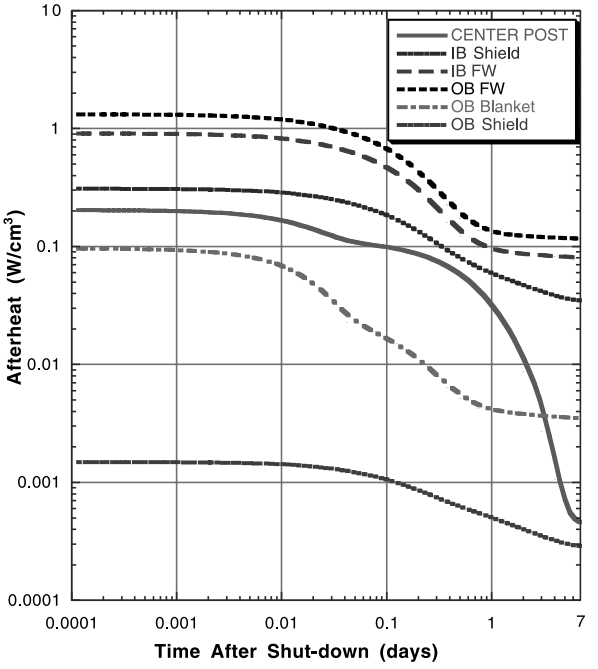

Fig. 6. Average specific decay heat in a 100% dense material at the midplane.

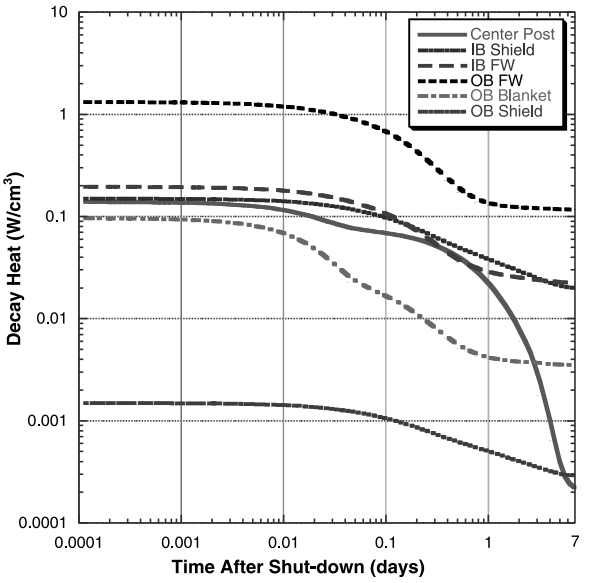

Fig. 7. Average specific decay heat in a 100% dense material behind the tungsten shielding plate.

and bottom. One can notice the effect of the additional shielding provided by tungsten on the decay heat induced in some of the plant components. The analysis also assumes a 1% conduction (1% of the facing area is thermally in physical contact with the other) in the gaps. The gaps are used to maintain the physical separation between the plant components at different temperature and they are also needed during maintenance. Table 4 shows a list of the initial thermal conditions used in the analysis.

4.3. Effect of thermal conductance through the gaps

In the ARIES-ST design, the gaps separating the plant components are used to maintain the physical separation between the different components operating at different temperatures. In addition, these gaps are also needed for the assembly of the plant components. Some physical contact between various surfaces must exist to keep the surfaces shape and to transfer structural loads between the different components. The heat leakage from various surfaces operating at different temperatures during normal operation is of a serious concern. A parametric analysis is performed to study the effect of thermal conductance through the gaps on the thermal response of the in-vessel components. A simplified 2-D finite-element (r,θ) model in cylindrical coordinates is employed for thermal analysis at the midplane is shown in Fig. 8. Various levels of partial thermal conduction through the gaps are used [12]. Fig. 9 shows the effect of thermal conductance through the gaps on the maximum temperature of outboard first wall. As shown in the figure, the slope of the temperature is very steep at lower values of conductance. Therefore, to minimize the heat leakage during normal operation, a reasonable value of 1% is chosen for the thermal conductance through the gaps.

Table 4
Initial thermal conditions (temperatures are in °C)

	T_{min}	T_{max}	T_{avg}
Outboard first wall			
He	300	425	362.5
Ferritic steel	300	600	450
Outboard blanket			
He in grid plates	425	500	462.5
Ferritic steel	450	550	500
$Li_{17}Pb_{83}$	500	700	600
Inboard first wall			
He	300	500	400
Ferritic steel	300	600	450
Inboard shield			
He	300	500	400
Ferritic steel	300	550	475
Centerpost			
Water	30	90	60
Copper	70	130	100
Divertor			
Tungsten	820		

4.4. Results and discussion

The temperatures of the various plant components were calculated as a function of time following a LOCA by using the transient thermal loads due to the decay heat, the assumed boundary conditions, and the initial temperatures of the various ARIES-ST components. The maximum temperature reached by the centerpost is 1018 °C. The maximum temperature of the inboard first wall is about 887 °C and the maximum temperature of the inboard shield is 974 °C. As shown in Fig. 10, these maximum temperatures are reached after 18 h from shutdown. As shown in Fig. 11, The maximum outboard first wall and blanket temperatures are 878 and 727 °C, respectively. The results showed elevated temperatures in the centerpost and an effective passive heat removal solution might be needed. Heat pipes can be used inside the centerpost to transfer the generated decay heat to the colder massive ends of the centerpost. In such a case, it is required to determine how many heat pipes are needed to reduce the maximum temperature of the centerpost and other plant components. Using heat pipes that occupy less than 5% of the centerpost total cross sectional area at the midplane would reduce the maximum temperature of centerpost, inboard first wall, and the inboard shield to less than 823, 803, and 828 °C, respectively. The maximum temperatures of outboard first wall and blanket would be also reduced to less than 796 °C and 682 °C, respectively [13].

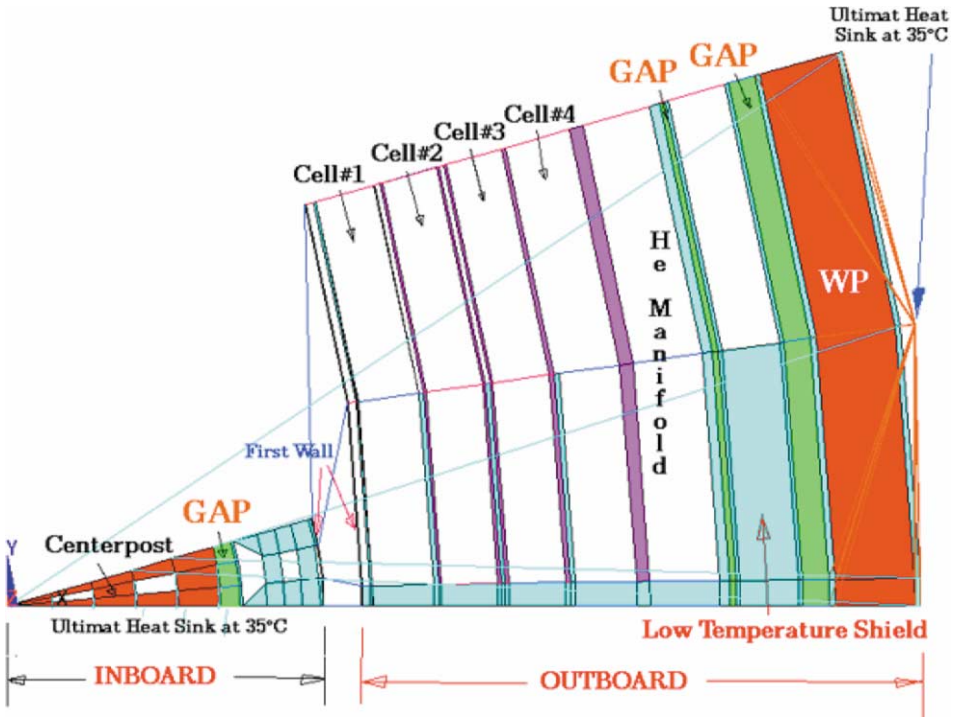

Fig. 8. Simplified finite element (r,θ) model for the inboard and outboard sides.

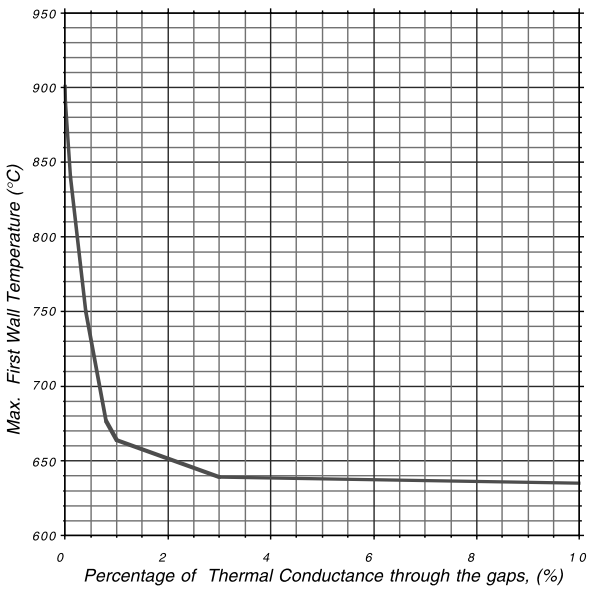

Fig. 9. Maximum temperature of the outboard first wall as a function of percentage of thermal conduction through the gaps.

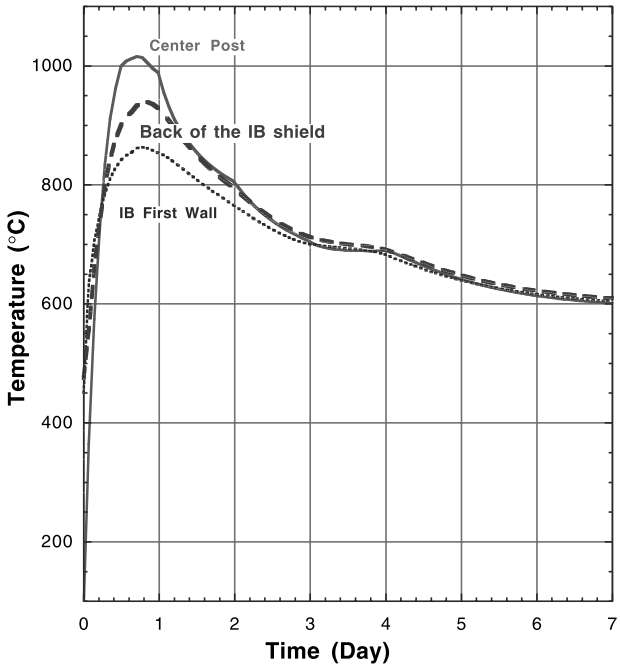

Fig. 10. Temperature variation history of the inboard components during the first week following a LOCA.

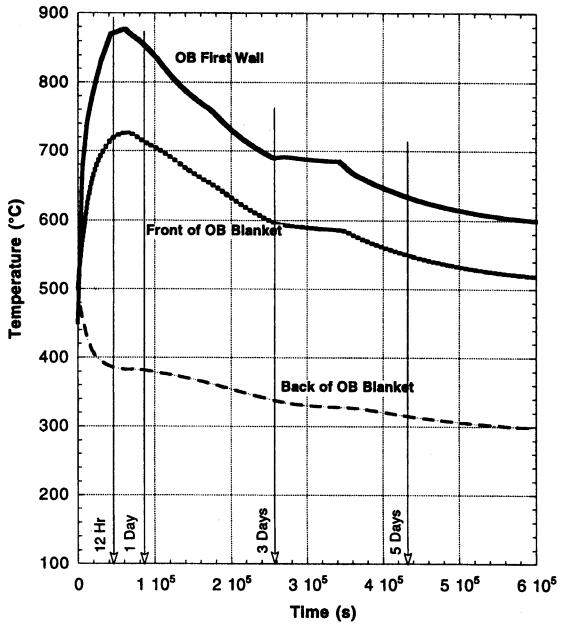

Fig. 11. Temperature variation history of the outboard components during the first week following a LOCA.

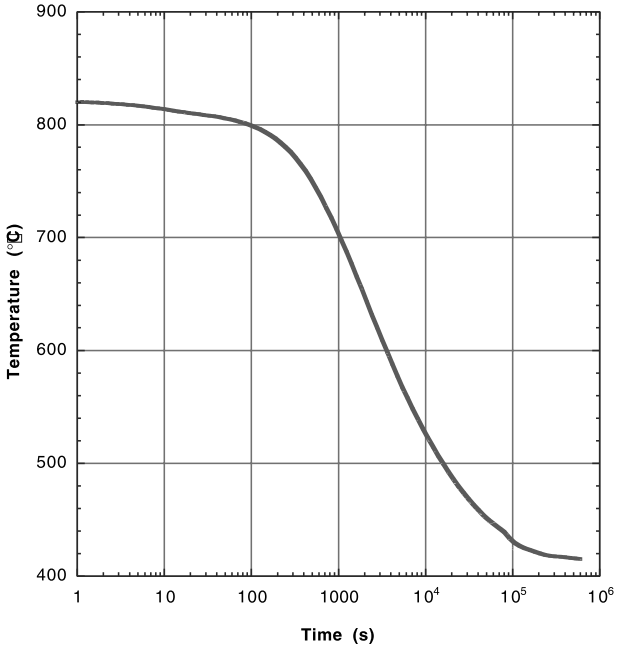

Fig. 12. Temperature variation of the divertor tungsten brush.

Finally, Fig. 12 shows the temperature variation of the divertor tungsten brush as a function of time following shutdown. The temperature drops quickly because of the large amount of steel in the back of the divertor plate that radiates to a colder surface at the top and the bottom of centerpost (100 °C).

5. Hazard assessment

5.1. Routine atmospheric effluents

The radiological dose to the population in the vicinity of the power plant site due to the routine release of tritium has been estimated by using the EPA AIRDOS-PC code. The code calculates the effective dose equivalent (EDE) as mandated by 40 CFR 61.93 and 61.94 to the maximally exposed individual and at several distances from the point of release. Dose values are computed from ingestion, inhalation, air immersion, and ground surface pathways. The routine releases from the several processing systems were based upon the quantity of tritium processed per day and followed experience at TSTA, which indicated that a barrier factor of 10^6 is an acceptable one. Assuming the release parameters listed in Table 5 and using meteorological conditions at different cities, we calculated the dose expected at typical locations near Boston, Chicago, Albuquerque and Los Angeles. A summary of the results is shown in

Table 5
Routine atmospheric release parameters

Site information	
Locations	Albuquerque, Boston, Chicago, Los Angeles
Temperature	15 °C
Rainfall	75 cm/y
Emission Information	
Year-round averaging	
Stack height	75 m
Stack diameter	30 cm
Momentum	1 m/s
Tritium pathways	
Steam generator	10 Ci/day
Total (adjusted for 80% availability)	2920 Ci/y

Table 6
Dose to the maximally exposed individual

Site	Dose (mrem/yr)	Distance (m)
Albuquerque	0.21	1000
Boston	0.09	3000
Chicago	0.13	1000
Los Angeles	0.28	3000

Table 6. The worst dose was in the Los Angeles area but was only 2.95 mrem/yr. More than 85% of the doses at all sites are incurred via the ingestion pathway. It is important to keep in mind that the estimated dose values strongly depend on the stack height. For example, using a 35-m stack height results in an EDE of 1.5 mrem/yr at the site boundary (1 km) if the Los Angeles meteorological conditions were used. Actually, the rule of thumb for determining the necessary stack height is to use 2.5 times the height of the nearest tall building in order to avoid downwash of the plume into the wake of the building [14]. A shorter stack must be justified with appropriate analysis.

5.2. Off-site dose calculations

A strong emphasis was given to the environmental and safety issues in the ARIES-ST design. Low activation ferritic steel (9Cr-2WVTa) was used in the first wall and shield to avoid generating high levels of induced radioactivity. Similarly, the use of $Li_{17}Pb_{83}$ as a breeder reduces the hazard posed by the energy producing chemical reactions usually associated with the use of lithium and hence reduces the risk of mobilizing the radioactive inventory present in the plant. To evaluate the possible radiological hazard to the public, a two-step approach was used in calculating the possible off-site dose. The first step in the approach is the identification of the sources and locations of the radioactive inventories inside the plant. However, since the existence of radioactivity does not in itself represent a safety hazard, the second step in the approach was to consider a pessimistic accident scenario for mobilizing and releasing the radioactive inventory. The analysis assumed a total LOCA as the worst case accident. During the LOCA, heat from all in-vessel components is transported to the massive copper busbars. In addition, in this analysis we also considered two possible scenarios during which radioactivity could be released from the divertor PFC. Following a disruption, off-site doses could be produced by direct vaporization of the divertor surface layer or by the release of tokamak dust. Tokamak dust (particles smaller than 100 μm in diameter) is produced by the vaporization of divertor surface material and accumulated during previous plasma disruptions.

The radioactive inventory calculated by the DKR-PULSAR2.0 code was used in conjunction with the isotope-specific dose data calculated by the MACCS code [15] to calculate effective whole body off-site dose inventory (dose caused by 100% release of radioactivity) under worst release conditions. These conditions are ground release, atmospheric stability class F, 1 km site boundary and 1 m/s wind speed. Doses calculated are produced through all of the following pathways:

- Inhalation of radionuclides during plume passage.
- Inhalation of resuspended radionuclides.
- External exposure to the plume.
- External exposure from ground deposition.
- Cloudshine or groundshine.
- Ingestion of contaminated food.

5.2.1. Off-site doses during a LOCA

During a LOCA, a large increase in the structure temperature could lead to the mobilization and partial release of the radioactive inventory. As previously discussed, the decay heat generated during the first day following a LOCA would increase the center post temperature by <1000 °C, the first wall/blanket temperature by <800 °C, and the divertor temperature by <800 °C. Under these conditions, the full mobilization of the structure radioactive products is impossible. The highest temperature the structure would reach determines the release fraction of its radioactive products (very conservative assumption).

Most of first wall/blanket radioactivity is generated in its steel component. Off-site dose calcu-

lations were performed using ferritic steel experimental volatility rates [16–18]. Low activation ferritic steel volatility rates at 700 °C in dry air were used in this analysis. To estimate conservative release fractions, a 24-h LOCA was assumed. The previously mentioned temperatures were assumed to last for 24 h and the voltilization rates were those found in 1-h experiments where no protective oxide has formed. Similar analyses (24-h LOCA) were performed for the centerpost and the divertor's tungsten PFC using experimental volatility rates for copper (using copper volatility rates at 1000 °C in dry air) and tungsten (using tungsten volatility rates at 800 °C in dry air), respectively.

The two sources of radiological hazard in a $Li_{17}Pb_{83}$ blanket are tritium and the activation products of $Li_{17}Pb_{83}$. As shown in Table 7, the steady state tritium inventory in $Li_{17}Pb_{83}$ is kept very low, on the order of 16 g, by its continuous removal during the plant operation. The activation products of major radiological hazard in a $Li_{17}Pb_{83}$ blanket are the two isotopes, ^{203}Hg ($T_{1/2} = 46.61$ d) and ^{210}Po ($T_{1/2} = 138.38$ d). Both ^{203}Hg (γ and β emitter) and ^{210}Po (α emitter) are highly volatile materials. Isotope ^{203}Hg produces a high prompt bone marrow dose and ^{210}Po results in high values of prompt, early as well as chronic doses. Isotope ^{210}Po is produced via nuclear transmutation of bismuth and is considered as the main safety hazard in $Li_{17}Pb_{83}$ blankets. Bismuth is a major impurity of commercial lead and is also produced as a transmutation product of Pb. Commercial Pb contains 500–1500 wppm of Bi and high-purity Pb contains less than 10 wppm of Bi. The $Li_{17}Pb_{83}$ used in this analysis contains 43 wppm of Bi impurities. It is desirable to keep the Bi impurity in lead below 10 wppm. The amount of Po generated can be controlled by limiting the Bi impurities initially present in Pb as well as the on-line continual removal of Bi atoms produced by neutron-lead reactions. Fortunately, Po evaporates into the form of an intermetallic compound PbPo, whose evaporation rates are very small because of the low vapor pressure of this polonide [19]. Similarly, Hg evaporates into the form of an intermetallic compound LiHg, whose evaporation rates are orders of magnitude lower that Hg [19]. It is estimated that Po retention in a $Li_{17}Pb_{83}$ melt is in the range of 96.4–99.2% [20]. In addition, under accidental spill conditions, the dilution of Po is such that α and γ radiation will be shielded by the large amount of lead atoms surrounding Po atoms.

A major advantage of using $Li_{17}Pb_{83}$ as a blanket is its low chemical reactivity. During an accident, leak of water into the $Li_{17}Pb_{83}$ region will result in a chemical reaction between water from the center post and the Li in the molten $Li_{17}Pb_{83}$ region. The reaction potential is much smaller than a water/liquid Li reaction. A $Li_{17}Pb_{83}$/water reaction tends to be self-limiting due to the fact that the liquid metal is formed by 83% Pb that does not react with water and which after initial depletion of Li, tends to shield the remaining amount of alloy from further interaction with water [19]. In addition, solid products Li_2O and LiOH are produced and provide shielding for the remaining liquid metal from the rest of the water. The $Li_{17}Pb_{83}$/water reaction is an exothermic reaction, which leads to an increase in temperature on the order of 200–400 °C. A complete reaction between water and $Li_{17}Pb_{83}$ would lead to the

Table 7
Tritium parameters

In $Li_{17}Pb_{83}$	
$Li_{17}Pb_{83}$ flow rate	47 450 kg/s
$Li_{17}Pb_{83}$ flow rate	2.5×10^5 mol/s
Sievert's constant at 700 °C	2×10^{-8} atom frac/Pa$^{0.5}$
Tritium source term	1.8×10^{-3} mol/s
Tritium concentration increase per coolant pass	7.2 appb
Tritium concentration in ARIES-ST	0.72 appm
Tritium partial pressure over $Li_{17}Pb_{83}$	7400 Pa
Estimated $Li_{17}Pb_{83}$ inventory	150 m^3
Total tritium inventory in $Li_{17}Pb_{83}$	16 g
In He	
He flow rate	1444 kg/s
He density at 500 °C	7.6 kg/m^3
He volumetric flow rate	190 m^3/s
Tritium source term	1.5×10^{-5} mol/s
Tritium pressure increase per coolant pass	0.005 Pa
Tritium pressure in He	5 Pa
Estimated He volume	200 m^3
Tritium inventory in He	1 g

production of 55.6 mole of H_2/kg of water. However, because the Li oxidation is the source of H_2 production, no oxygen is present and therefore explosion cannot occur [21].

The off-site doses were calculated by combining the total off-side dose inventory with the different volatility data under the LOCA condition discussed previously. Since no volatility data are available for $Li_{17}Pb_{83}$, very conservative release rates were adopted for the release of ^{3}H, ^{203}Hg and ^{210}Po. All of the ^{3}H, 30% of the ^{203}Hg and 10% of the ^{210}Po were assumed to mobilize during an accident. Minor air ingress into the coolant channel results in the volatilization of in-vessel materials as previously discussed. Once airborne, these particles could be transported to the site boundary. Assuming that the vacuum vessel and the containment would stay intact during accidents, they would be expected to act as release barriers. For a vacuum vessel leak rate of 1% per day, a containment factor of 99% could be considered. Considering the vacuum and containment boundaries as two independent barriers leads to an overall radioactivity containment factor of 99.99% [22–24]. As shown in Table 8, the LOCA based accident produces an effective whole body early dose of 1.88 mSv at the site boundary.

5.2.2. *Off-site doses due to divertor disruption*

Assumptions used for the energy dissipated in the divertor during a disruption are similar to assumptions used in the International Thermonuclear Experimental Reactor safety analysis [25]. Following a disruption, off-site doses could be produced by direct vaporization of the divertor surface layer. The total energy dissipated during the energy quench phase is 2.1 GJ. During a disruption, very small particles (0.1 μm) are mobilized by direct vaporization. Assuming an interaction surface area of 15 m^2, the total amount of tungsten vaporized during a disruption is 1 kg [20]. In addition, tokamak dust (particles smaller that 100 μm in diameter) is produced by the vaporization of the divertor surface material and accumulated during previous plasma disruptions. This dust could be mobilized during an accident or during in-vessel maintenance. Assuming an interaction surface area of 15 m^2, the total amounts of tungsten vaporized and melted during a disruption are 1.16 and 60.8 kg, respectively. All of the vaporized tungsten and 10% of the melted tungsten (melt layer splash) are assumed to form dust resulting in the total production of 7.24 kg of tungsten per full-power disruption [26]. As shown in Table 9, considering the vacuum and containment boundaries as two independent barriers with an overall radioactivity containment factor of 99.99%, the divertor disruption would only produce an effective whole body early dose of 7.68 μSv at the site boundary.

One of the issues that needs to be addressed in a future analysis is the impact of the divertor shape on the amount of material vaporized during disruption. Because of the narrow V-shape (closed) of the ARIES-ST divertor, the radiation energy (photons) from the vapor cloud (the vapor shielding area) will be deposited on near surface area causing significantly higher additional erosion [26]. Taking the vapor cloud effect into account could increase the amount of dust generated by as

Table 8
Early doses released during a severe LOCA

Zone	Inventory (Sv)	Mobilized inventory (Sv)	Released (mSv)	Dominant nuclides
Centerpost	2502	1.1	0.11	^{60}Co
Inboard shield	4175	1.7	0.17	^{60}Co, ^{54}Mn, ^{56}Mn
Inboard first wall	306	0.2	0.02	^{54}Mn, ^{56}Mn, ^{60}Co
Outboard first wall	5000	2	0.2	^{54}Mn, ^{56}Mn, ^{60}Co
Blanket	2257	13.8	1.38	^{210}Po, ^{203}Hg, ^{54}Mn
Manifold	167	0.04	0.004	^{60}Co
Outboard shield	53	0.008	0.0008	^{60}Co
Divertor plate	77.8	0.004	0.0004	^{187}W, ^{181}W, ^{185}W

Table 9
Early doses released during a disruption

Pathway	Inventory (Sv)	Mobilized inventory (Sv)	Released (mSv)	Dominant nuclides
Direct vaporization	79.4	10.6	1.06	^{187}W, ^{181}W, ^{185}W
Tokamak dust	54.8	66.2	6.62	^{187}W, ^{181}W, ^{185}W

much as an order of magnitude more than the values reported in Table 9.

6. Summary and conclusions

Detailed activation and safety analyses were performed for the ARIES-ST spherical tokamak power plant. ARIES-ST includes a water-cooled copper centerpost and uses a $SiC/Li_{17}Pb_{83}$ blanket. The plant is assumed to operate for 40 FPY. Neutron irradiation resulted in the increase of the centerpost copper resistivity due to the production of neutron-induced transmutation. Neutron transmutation of copper resulted in the production of several nickel, cobalt and zinc isotopes. The production of these isotopes resulted in an increase of the time-space average resistivity of the centerpost by as much as 6% after 2.86 FPY. Waste disposal limits were calculated for the different plant components using the NRC 10CFR61 and Fetter waste disposal limits. All of the plant components met the limits for disposal as Class C LLW. The decay heat generated during the first day following a LOCA would increase the centerpost temperature by <1000 °C, the first wall/blanket temperature by <800 °C and the divertor temperature by <800 °C. The calculated temperature profiles and available oxidation-driven volatility experimental data were used to calculate doses at the site boundary under conservative release conditions. The vacuum vessel and the containment were assumed to stay intact during accidents and hence act as release barriers. A leak rate of 1% per day and a containment factor of 99% were considered for each of the two barriers. The current design produces an effective whole body early dose of 1.88 mSv at the site boundary. Finally, a divertor disruption would only produce an effective whole body early dose of 7.68 μSv at the site boundary.

Acknowledgements

Support for this work was provided by the US Department of Energy.

References

[1] F. Najmabadi, The ARIES Team, Overview of ARIES-ST spherical torus power plant study, Fusion Eng. Des., this issue.
[2] M.S. Tillack, X.R. Wang, J. Pulsifer, et al., Fusion power core engineering for the ARIES-ST power plant, Fusion Eng. Des., this issue.
[3] L.A. El-Guebaly, The ARIES Team, ARIES-ST Nuclear Analysis and Shield Design, this issue.
[4] R. O'Dell, et al., User's Manual for ONEDANT: A Code Package for One-Dimensional, Diffusion-Accelerated, Neutral Particle Transport, Los Alamos National Laboratory report, LA-9184-M (1982).
[5] R. MacFarlane, FENDL/MG-1.0, Library of Multigroup Cross Sections in GENDF and MATXS formet for Neutron-Photon Transportat Calculations, Report IAEA-NDS-129, Rev. 2, International Atomic Energy Agency (April 1995).
[6] J. Sisolak, Q. Wang, H. Khater, D. Henderson, DKR-PULSAR2.0: A Radioactivity Calculation Code that Includes Pulsed/Intermittent Operation, in press.
[7] A. Pashchenko, et al., FENDL/A-2.0: Neutron Activation Cross-Section Data Library for Fusion Applications, International Atomic Energy Agency report IAEA-INDC (NDS)-173, IAEA Nuclear Data Section, (March 1997).
[8] User's Guide for AIRDOS-PC, Version 3.0, US Environmental Protection Agency report EPA 520/6-89-035, EPA Office of Radiation Programs, Las Vegas, NV (December 1989).
[9] US Nuclear Regulatory Commission, 10CFR part 61, Licensing Requirements for Land Disposal of Radioactive Waste, Federal Register, FR 47, 57446 (1982).
[10] S. Fetter, E. Cheng, F. Mann, Long term radioactive waste from fusion reactors, Fusion Eng. Des. 13 (1990) 239–246.

[11] ANSYS 5.4 User's Manual, Updo, DN-R300:50–2 (1992).
[12] E.A. Mogahed, The ARIES Team, Loss of Coolant Accident (LOCA) Analysis of the ARIES-ST Design, Proceedings of the ANS 13th Top. Mtg. Technol. of Fusion Energy, Nashville, TN, June 1998, Fusion Technol. 32 (1998).
[13] E.A. Mogahed, Heat Pipes Analysis Applied to ARIES-ST Centerpost, in press.
[14] US Nuclear Regulatory Commission, Regulatory Guide 1.145/Rev.1 (Feb. 1983).
[15] D.I. Chanin, et al., MELCOR Accident Consequences Code System (MACCS), vol. 1–3, NUREG/CR-4691, SAND86-1562 (Feb. 1990).
[16] K.A. McCarthy, G.R. Smolik, S.L. Harms, A Summary and Assessment of Oxidation Driven Volatility Experiments at INEL and Their Application to Fusion Reactor Safety Assessments, Idaho National Engineering Laboratory report EGG-FSP-11193 (Sep. 1994).
[17] K.A. McCarthy, M.J. Gaeta, Activation Source Term Input for ESECS, Idaho National Engineering Laboratory Design File ITER/US/95/TE/SA-6 (June 1995).
[18] K.A. McCarthy, Activation Product Source Term for NSSR-1, Idaho National Engineering Laboratory Design File ITER/US/95/TE/SA-10 (July 26, 1996).
[19] L.J. Wittenberg, University of Wisconsin-Madison, private communications, January 1998.
[20] N.J. Hoffman, et al., Polonium aspects associated with the use of lead-lithium blankets in fusion applications, Fusion Technol. 8 (1985) 1376.
[21] L. Giancarli, M.A. Fütterer, Water-Cooled Pb-17Li DEMO Blanket Line, Status Report on the Related EU Activities, CEA Report, SERMA/LCA/1801 (1995).
[22] N.P. Taylor, et al., Safety and environmental assessment of a variety of blanket concepts and structural materials, Proceedings of the 19th Symposium on Fusion Technology (SOFT), Lisbon, Portugal, September 16–20, 1996.
[23] D.A. Petti, Estimates of Activation Product Transport through ITER Confinements, Idaho National Engineering Laboratory Design File ITER/US/94/EN/SA-7, May 6, 1994.
[24] D.A. Petti, D.L. Hagrman, Estimates of Activation Product Transport through ITER Confinements, Proceedings of the ANS 12th Top. Mtg. Technol. of Fusion Energy, Reno, NV, (June 1996), Fusion Technol. 30 (1996).
[25] ITER, Non-Site Specific Safety Report, vol. 3, IAEA, (December 1997).
[26] A. Hassanein, Argonne National Laboratory, private communications, November 1998.